buildings

MDPI

Article

Blast-Induced Dynamic Response and Vibration Control of an Existing Water Diversion Tunnel During Adjacent Tunnel Excavation

Sichang Wang, Jingren Tian *, Baopeng Yang and Qiang Fu

School of Civil Engineering, Chongqing University of Science and Technology, Chongqing 401331, China; 2011015@cqust.edu.cn (S.W.); 2024206080@cqust.edu.cn (B.Y.); 2023206065@cqust.edu.cn (Q.F.)
* Correspondence: 2025207029@cqust.edu.cn

Abstract

Blasting excavation of adjacent tunnels can induce significant vibrations in existing underground structures under complex spatial constraints. This study investigates the dynamic response and vibration control of an existing water diversion tunnel subjected to blasting-induced disturbances from an adjacent tunnel. Field monitoring, three-dimensional numerical simulation, and blasting parameter optimization were integrated to reveal the vibration characteristics and control mechanisms. The propagation characteristics of blasting vibrations were first analyzed based on field measurements. A three-dimensional dynamic model was then established using MIDAS GTS NX and validated against the monitoring results. The vibration velocity, displacement response, and stress evolution of the existing tunnel lining were systematically investigated. Results indicate that vertical vibration dominates the dynamic response, while stress evolution reflects the propagation, energy transfer, and dissipation processes of blasting stress waves. Furthermore, entropy weight–gray relational analysis identified six key factors influencing blasting vibration. Based on these factors, blasting parameters were optimized by reducing energy concentration. Field verification demonstrated reductions of 11.05%, 10.69%, and 21.54% in vibration velocities along the X, Y, and Z directions, respectively. This study provides insights into vibration response mechanisms and effective control strategies for similar underground engineering projects.

Keywords: tunnel blasting; existing diversion tunnel; dynamic response; vibration control; numerical simulation; blasting parameter optimization

Check for updates

Academic Editor: Fabrizio Gara

Received: 25 August 2026
Revised: 10 October 2026
Accepted: 15 October 2026
Published: 22 October 2026

Copyright: © 2026 by the authors. Licensee MDPI, Basel, Switzerland. This article is an open access article distributed under the terms and conditions of the Creative Commons Attribution (CC BY) license.

1. Introduction

1.1. Research Background

With the continued development of transportation, water conservancy, and energy infrastructure, newly constructed tunnels are increasingly required to pass close to or intersect existing underground structures. Drill-and-blast excavation remains widely used in rock tunneling because of its high efficiency and adaptability to complex geological conditions. However, blasting generates transient stress waves that propagate through the surrounding rock and may induce vibration, displacement, and stress responses in nearby underground structures. Such effects become particularly important when a newly excavated tunnel crosses an existing water diversion tunnel at a short distance, where the restricted propagation path and complex spatial relationship between the two structures

may intensify the local dynamic response. Previous field investigations have shown that blasting excavation near existing water diversion tunnels can produce measurable structural vibration and therefore requires appropriate safety assessment and vibration control [1]. Accordingly, clarifying the dynamic response of existing water diversion tunnels and establishing effective mitigation measures are important for ensuring construction safety under close-crossing conditions.

The propagation and attenuation of blast-induced vibration have been extensively investigated. Peak particle velocity (PPV) is commonly used as a principal indicator for evaluating blasting vibration, and its attenuation is closely related to charge weight, blast-source distance, free-surface condition, and characteristics of the surrounding medium [2–4]. Recent studies have further emphasized that attenuation parameters may exhibit substantial variability under different site conditions, highlighting the importance of project-specific calibration rather than direct transfer of empirical coefficients between engineering sites. In addition to vibration amplitude, the frequency characteristics of blasting waves have received considerable attention. Studies on millisecond-delay tunnel blasting have demonstrated that vibration frequency and wave superposition are affected by the initiation sequence and delay characteristics [5]. Time-frequency analyses of tunnel blasting signals have also provided additional information for characterizing the transient response of surrounding rock and nearby structures [6]. These studies have substantially advanced understanding of blast-wave propagation; nevertheless, most investigations focus on vibration characteristics or attenuation behavior themselves, whereas the coupled process linking blast-source characteristics, wave propagation, and structural response under close tunnel-crossing conditions still warrants systematic analysis.

The dynamic response of adjacent underground structures subjected to blasting has also been investigated using field monitoring and numerical simulation. Experimental and numerical studies have addressed the influence of blasting from adjacent tunnels on existing tunnel structures [7], while other research has examined vibration velocity and frequency characteristics in surrounding rock during adjacent-tunnel excavation [8]. For water diversion tunnels, stability under short-distance blasting excavation has also been assessed [9]. In addition, the influence of a newly constructed tunnel on an existing tunnel under a small crossing angle has been investigated numerically [10]. Collectively, these studies confirm the importance of geometric configuration and close-proximity effects in evaluating blast-induced structural responses. However, many existing studies primarily emphasize PPV, vibration frequency, safety distance, or representative structural responses. For a newly constructed tunnel passing above an existing water diversion tunnel, the combined spatial and temporal evolution of vibration velocity, displacement, and stress, together with their relationships to controllable blasting parameters, has not yet been fully integrated within a unified engineering analysis framework.

Blast-induced vibration is generally controlled by reducing the charge weight per delay, optimizing blast-hole arrangements, adjusting delay intervals, and redistributing explosive energy. Previous studies have explored vibration reduction through blasting-parameter adjustment and refined blasting techniques [11]. The influence of different vibration-control factors and the optimization of mitigation measures for adjacent-tunnel blasting have also been investigated [12]. Spectrum-based approaches have further demonstrated the potential of controlling vibration superposition through appropriate initiation design [13], while recent tunnel studies have incorporated both vibration reduction and excavation-profile control into blasting-parameter optimization [14]. These studies provide useful strategies for vibration mitigation. Nevertheless, in close crossing projects, several parameters—including blast-source distance, total charge, maximum charge per delay, maximum charge in cut holes, number of blast holes, and delay arrangement—may simul-

taneously influence the measured vibration response. Consequently, parameter adjustment based mainly on engineering experience makes it difficult to distinguish the relative importance of individual factors. Moreover, identifying which parameter is important does not directly determine the quantitative level to which that parameter should be controlled. A more systematic strategy is therefore required to link influencing-factor identification with quantitative safety constraints and subsequent engineering verification.

1.2. Research Objectives

To address these issues, this study investigates the newly constructed Miaolin Tunnel of the Maliuwan–Yiliang Expressway, which passes above an existing water diversion tunnel of the Miaolin Hydropower Station under Class V surrounding-rock conditions. The study integrates field monitoring, three-dimensional numerical simulation, entropy-weighted gray relational analysis, blast-vibration attenuation analysis, and blasting-parameter optimization. Rather than treating these methods independently, they are organized into a sequential framework of response characterization, quantitative identification of key influencing factors, determination of safety constraints, targeted parameter optimization, and field verification. The main contributions of this study are as follows:

1. Dynamic-response characterization under close-crossing conditions. Three-directional vibration velocities and dominant frequencies of the existing water diversion tunnel are obtained through field monitoring. A three-dimensional numerical model incorporating the newly constructed tunnel, surrounding rock, and existing water diversion tunnel is then established and validated against the measured data. The spatial distribution and temporal evolution of vibration velocity, displacement, and first principal stress are subsequently analyzed to characterize the dynamic response of the existing tunnel lining.
2. Quantitative identification of the principal controllable factors. Based on the physical sequence of blast generation, wave propagation, and structural response, the principal blasting-related variables are selected and evaluated using entropy-weighted gray relational analysis. Their relationships with dominant frequency, PPV, and vibration duration are quantified to distinguish parameters that are both influential and practically adjustable, thereby providing a quantitative basis for targeted optimization.
3. Integration of factor identification, safety constraints, and engineering verification. Because influence-factor ranking alone cannot provide an allowable control value for key blasting parameters, field monitoring data are further used to establish a project-specific blast-vibration attenuation relationship and determine the allowable maximum charge per delay under the examined close-crossing condition. The blasting scheme is subsequently optimized within this constraint and evaluated through numerical simulation, field trial blasting, and monitoring during construction through the critical crossing section.

Through this framework, the study aims to clarify the blast-induced dynamic response of an existing water diversion tunnel under close-crossing conditions and to develop a practical vibration-control procedure linking dynamic-response assessment, key-factor identification, quantitative safety constraint, blasting-parameter optimization, and field validation. The findings are expected to provide a technical reference for blasting construction near similar existing underground structures.

1.3. Research Flowchart

The research flowchart is shown in Figure 1.



Figure 1. Research flowchart.

2. Materials and Methods

2.1. Engineering Background and Case Description

This study focuses on the Miaolin Tunnel of the Maliuwan–Yiliang Expressway in Longtan Village, Zhongming Town, Yiliang County, Yunnan Province. The adjacent water diversion tunnel passes beneath the newly constructed Miaolin Tunnel near the surveying and design mileage K21 + 166; the spatial intersection range between the new Miaolin Tunnel and the existing water diversion tunnel is from K21 + 73 to K21 + 166. The Miaolin Tunnel adopts a separated double-tunnel design, and during the construction of both the left and right tunnels, they form a close-proximity spatial intersection with the existing water diversion tunnel, as shown in Figure 2.

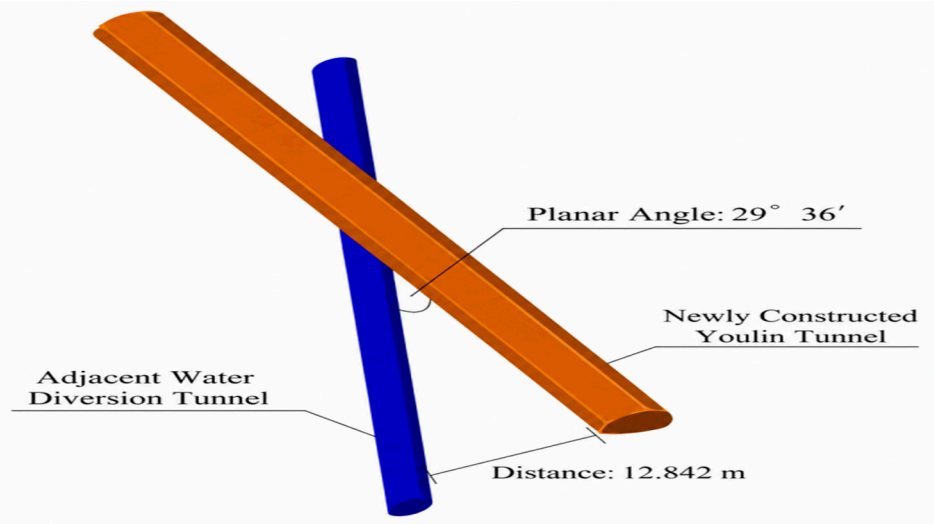


Figure 2. Schematic diagram of the positional relationship between the newly constructed tunnel and the adjacent water diversion tunnel.

Due to the small distance between the two tunnels, vibration waves generated by blasting are affected by the spatial relationship and propagation path within the surrounding rock as they propagate, subsequently impacting the surrounding rock and lining structure of the adjacent diversion tunnel and inducing dynamic responses.

The geological conditions in the study area are relatively complex; the tunnel surrounding rock mainly consists of Quaternary overburden and the Feixianguan Formation bedrock of the Lower Triassic system, with hard rock predominating overall. Joint and fracture development is observed in certain localized areas. The structural characteristics of the surrounding rock influence the propagation process of blasting vibrations and the attenuation pattern of vibration energy. The newly constructed Miaolin Tunnel employs a composite lining structure, while the adjacent diversion tunnel is an underground water conveyance structure in long-term operation. In this project, the blasting construction of the new tunnel and the existing diversion tunnel have a close spatial relationship, exhibiting typical characteristics of blasting effects on adjacent underground structures. This makes it suitable for studying the propagation of blasting vibrations and the dynamic response of structures under complex spatial conditions.

2.2. Field Monitoring Program

To investigate the vibration effects of blasting construction for a newly built tunnel on an adjacent existing water diversion tunnel, on-site blasting vibration monitoring was carried out during the construction process. Field monitoring was conducted in the K21 + 73~K21 + 98 intersection influence section to collect dynamic response data such as three-dimensional vibration velocity and the dominant vibration frequency of the water diversion tunnel lining. These data were evaluated according to the Safety Regulations for Blasting (GB 6722-2014) [15] to identify the characteristics and distribution patterns of excessive vibrations under the original blasting plan, providing empirical evidence for subsequent research. Field vibration monitoring has been widely applied to evaluate and control blast-induced vibration in diversion and transportation tunnels [16,17].

Monitoring was carried out on-site using the YT-BP-01 type blasting vibration monitor (Jiangsu Yantai Engineering Instrument Co., Ltd., Danyang, China), which can simultaneously collect vibration velocity responses in three directions. The monitor was installed on the lining surface of the existing water diversion tunnel to continuously capture the vibration responses during blasting operations. The vibration monitoring system triggers

at a vibration velocity threshold of 0.1 cm/s, with a single sampling duration of 5 s and a sampling interval of 1 ms. The monitored parameters mainly include the vibration velocity components in three directions and the dominant vibration frequency, which are used to analyze the vibration response characteristics of the existing tunnel structure under blasting effects.

Based on the spatial relationship between the newly constructed tunnel and the existing diversion tunnel, as well as the characteristics of blasting vibration propagation, monitoring points were arranged in the lining area of the diversion tunnel affected by blasting excavation. The measuring points were positioned along the longitudinal axis of the diversion tunnel directly beneath the blasting face of the new tunnel, with a longitudinal spacing of 5 m to determine the variation pattern of vibration velocity with propagation distance. Due to limitations imposed by on-site construction conditions and the installation requirements of the tunnel lining, the monitoring points were ultimately placed on the sidewalls of the diversion tunnel at a height of 1.2 m above the tunnel floor.

The monitoring scheme comprehensively considers the location of the explosion source, the spatial relationship of the tunnel, and the characteristics of blasting vibration propagation. The on-site monitoring data are used for subsequent analysis of blasting vibration characteristics and provide a basis for the verification of numerical simulation results.

The installation and deployment of blasting vibration monitors need to be carried out in an orderly manner according to standardized procedures: First, the selection of installation locations should be carried out, and after marking, drilling should be carried out. Then, the bracket should be installed and adjusted to a horizontal state to provide a solid foundation for the installation of the monitor. Next, install the blasting vibration monitor and power supply equipment in sequence, accurately connect the airline cables, and ensure that the plugs are fully inserted to build a stable circuit connection; Afterwards, the equipment is started, and after confirming that the power supply is normal, it is switched to the adaptive working mode. The test is conducted by tapping the wall near the equipment to simulate a vibration scenario, and the data is viewed synchronously on the platform to verify the equipment's function of collecting and transmitting vibration information. Finally, a protective cover is installed to fully complete the installation and commissioning of the monitoring equipment, providing a guarantee for its continuous and stable collection and transmission of vibration data in the blasting operation environment. Since this project is located in a weak-signal area, a Wi-Fi communication upload gimbal mode is adopted.

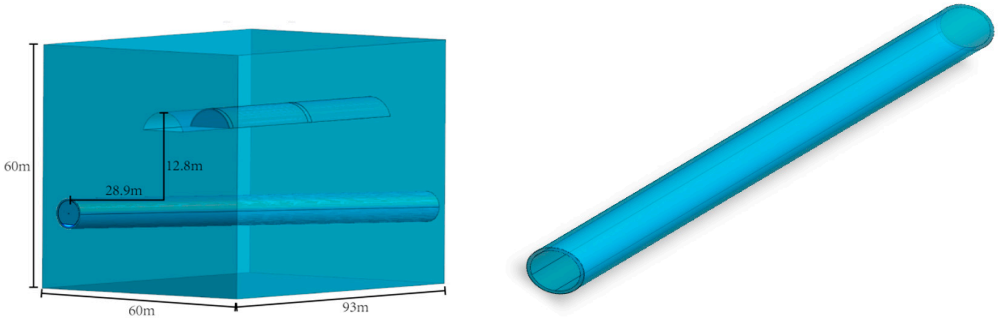
The longitudinal spacing between monitoring points is determined based on the actual construction conditions at the site. For areas adjacent to the lining walls of the diversion tunnel affected by blasting operations in the newly constructed tunnel, monitoring points for blasting vibration are arranged along the longitudinal axis of the diversion tunnel directly beneath the blasting face of the new tunnel at 5 m intervals. This spacing is set according to the wavelength of the propagating blast stress wave, enabling effective capture of the dynamic variation characteristics of peak vibration velocity. However, due to limited working space above the tunnel, the uneven surface caused by the curved structure of the lining, and instability resulting from the mechanical characteristics of the overhead lining, it is impossible to install sensors at their theoretically optimal positions. Considering the site conditions and structural stress characteristics, the monitoring points are ultimately placed on the side walls along the tunnel cross-section, at a height of 1.2 m above the tunnel floor. For each blasting operation, 3–6 monitoring points are deployed; the exact number can be adjusted flexibly according to on-site construction conditions. Each point is equipped with a triaxial blasting vibration sensor to simultaneously collect vibration components in

the X, Y, and Z directions, allowing for concurrent monitoring of vertical and horizontal vibration parameters. The longitudinal spacing between monitoring points is determined dynamically according to the construction progress, and the sensors are securely fixed to the lining surface using embedded parts or specialized mounting brackets. Blasting vibration velocity and acceleration are automatically recorded by a blasting vibration recorder to analyze vibration waveforms and attenuation patterns.

2.3. Numerical Model Establishment

2.3.1. Model Geometry and Numerical Scheme

In order to study the dynamic response characteristics of new tunnel blasting construction to adjacent existing diversion tunnels, based on the actual engineering conditions of the K21 + 104~K21 + 166 cross-influence section of Miaolin Tunnel, a three-dimensional dynamic numerical model was established using MIDAS GTS NX, a finite element software for geotechnical tunnel engineering. The model is shown in Figure 3.



(**a**) Schematic diagram of 3D model (**b**) Schematic diagram of adjacent diversion tunnel

Figure 3. Schematic diagram of 3D model.

The model comprehensively considers the spatial relationship between the new tunnel, the existing diversion tunnel, and the surrounding rock mass, and establishes a calculation model including the surrounding rock medium, the new tunnel, and the existing diversion tunnel structure. By simulating the propagation process of stress waves in the surrounding rock under blasting load, the dynamic response characteristics of the adjacent diversion tunnel structure are analyzed, which provides a calculation basis for subsequent vibration response analysis and optimization of blasting parameters.

2.3.2. Material Properties and Boundary Conditions

Through on-site engineering data investigation, it can be found that the intersection of the newly built tunnel and the adjacent diversion tunnel is mainly lithologically based on quartz sandstone, and the surrounding rock grade is grade V; The adjacent diversion tunnel is lined with C30 concrete with a thickness of 50 cm; Three-dimensional solid elements are used in the surrounding rock and lining elements in the numerical simulation. The calculated parameters of this model are shown in Table 1.

Table 1. Finite element model parameter table.

Material Type	Elastic Modulus (GPa)	Unit Weight (KN/m^3)	Poisson's Ratio	Cohesion (KN/m^2)	Friction Angle φ (°)	Surrounding Rock Grade
Quartz sandstone	20	24.5	0.3	200	25	V
Lining of the adjacent diversion tunnel	30	25	0.2	/	/	/

In terms of the water level setting of the diversion tunnel, the water level setting of the diversion tunnel is included in the Midas working condition setting. Because the water level of the diversion tunnel is low during construction, the water level of the diversion tunnel measured on site during construction is 0.3~0.5 m, and the average value of 0.4 m is taken as the simulated value, and hydrostatic pressure is applied accordingly.

In order to reduce the influence of reflection and refraction of blasting seismic waves propagating to the model boundary on the calculation results, viscous boundary conditions are adopted for dynamic time history analysis. Horizontal and vertical fixed constraints are applied at the bottom of the model, and point springs are set at the cell nodes; the Lysmer–Wass viscous boundary is used for the lateral boundary of the model. The boundary parameters are calculated according to the corresponding stiffness relationship in the original model:

$$c_p = \rho A\sqrt{\frac{\lambda + 2G}{\rho}} = \omega A\sqrt{\frac{\lambda + 2G}{9.81\omega}} = c_p A$$

$$c_s = \rho A\sqrt{\frac{G}{\rho}} = \omega A\sqrt{\frac{2G}{9.81\omega}} = c_s$$

$$\lambda = \frac{\nu E}{(1+\nu)(1-2\nu)}$$

$$G = \frac{E}{2(1+\nu)}$$

where λ is the first Lamé constant (Pa); G is the shear modulus (Pa); E is the elastic modulus (Pa); ν is Poisson's ratio; and A is the cross-sectional area (m^2).

In the formula, the meaning and unit of each parameter are defined according to the original model. Through the above-mentioned boundary setting, the influence of artificial boundary reflected waves on the blasting vibration propagation process is reduced.

2.3.3. Blast Loading and Simulation Conditions

To ensure that the input of numerical simulation blasting loads matches the actual construction conditions, the model blasting parameters were determined based on the actual blasting plan for the intersection section of Miaolin Tunnel and the diversion tunnel. As shown in Table 2, the surrounding rock in the study area is classified as Grade V, and a three-bench controlled blasting method was employed for excavation. The diameter of blast holes in each bench is 42 mm, with a cyclic advance of 1.2 m. The upper bench uses a combination of inclined and vertical cut patterns for hole arrangement, while the middle and lower benches have collapse holes, inner-circle holes, and perimeter holes arranged according to excavation conditions. Non-electric composite detonation methods were used on-site, with different delay detonators controlling the firing sequence of blast holes to reduce the cumulative effect of blasting vibrations. A total of 137 blast holes were arranged in one blasting operation, with a total explosive charge of 47.8 kg; among them, there are 14 cut holes in total.

To reduce the computational cost associated with explicit modeling of individual blast holes, the blasting load was equivalently applied based on Saint-Venant's principle and commonly adopted blasting-load treatment approaches [18,19]. Ignoring the actual geometry of the borehole, the blasting effect is approximated as a concentrated dynamic load, which is applied to the corresponding blasting area in the form of pressure, with the load direction perpendicular to the acting surface, as shown in Figure 4.

Table 2. Main blasting parameters used in the numerical simulation.

Parameter	Value
Surrounding rock grade	Class V
Excavation method	Three-bench controlled blasting
Blast hole diameter	42 mm
Advance per round	1.2 m
Cut hole arrangement	Inclined cut holes combined with straight cut holes
Total number of blast holes	137
Total explosive charge	47.8 kg
Number of inclined/straight cut holes	14
Initiation method	Non-electric millisecond initiation
Delay mode	Multi-stage delay blasting

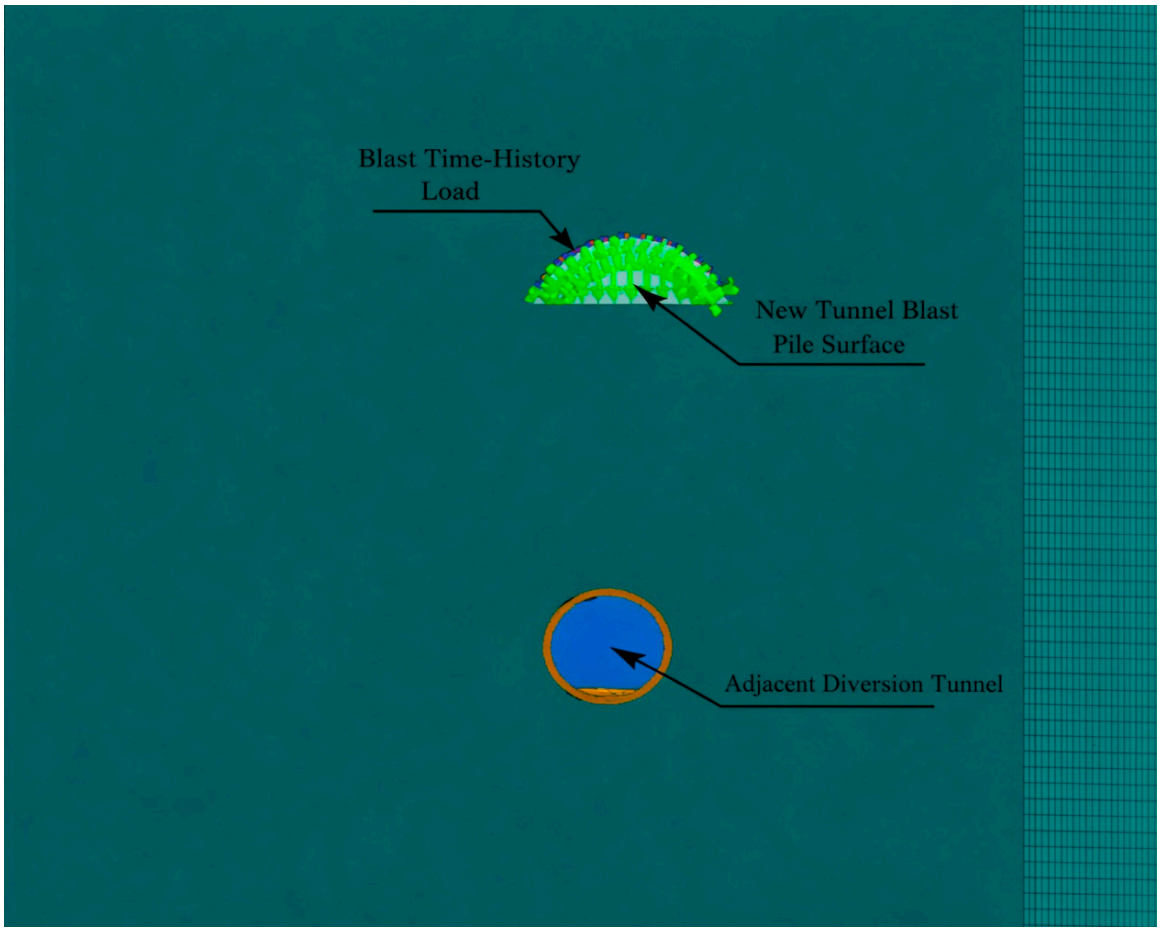


Figure 4. Schematic diagram of blasting load application.

The blasting load time history is described using a triangular pressure-time curve, as shown in Figure 5, with the peak pressure determined based on blasting load calculation methods, combined with the detonation characteristics of explosives, surrounding rock conditions, and on-site blasting parameters. Based on the blasting construction parameters under Class V surrounding rock conditions, dynamic load inputs corresponding to the actual blasting process are established. Subsequently, the dynamic time-history analysis method is employed to simulate the propagation of blasting vibrations in the surrounding rock and to analyze the dynamic response characteristics of the adjacent diversion tunnel structure under blasting disturbance.

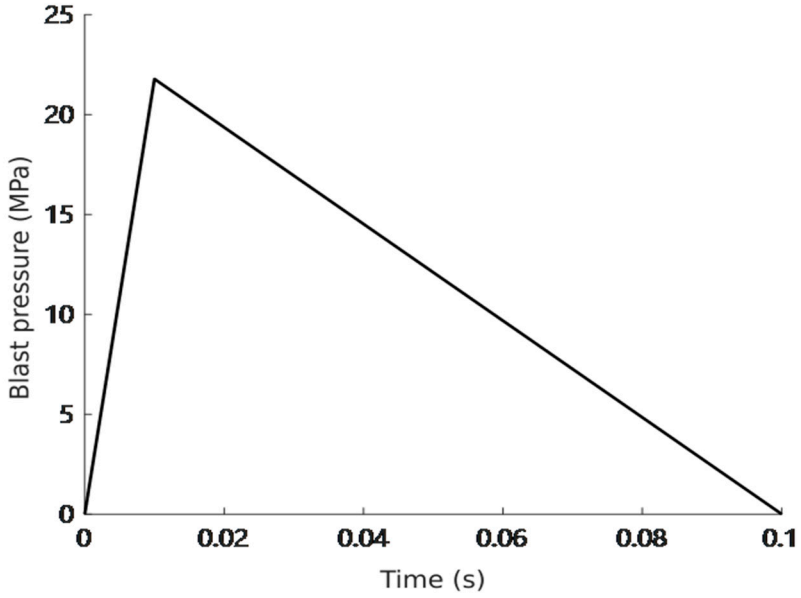


Figure 5. Schematic diagram of triangular blast load application curve.

The established numerical model is then validated using on-site monitoring data, and the validation results will be discussed in Section 3.2.

3. Results and Discussion

3.1. Field Monitoring Results and Vibration Characteristics

Based on the field blasting vibration monitoring results, the vibration response of the adjacent existing water diversion tunnel under the blasting construction conditions of the newly built Miaolin Tunnel was analyzed. The construction crossover section is from K21 + 73 to K21 + 166; the typical three-dimensional vibration velocities and vector-combined waveforms at the right wall of the water diversion tunnel during the blasting construction at K21 + 73 of the right tunnel of the new tunnel were selected for analysis, as shown in Figure 6.

The typical vibration waveform shows significant differences in the peak vibration velocities among the three directions. The peak values in the X, Y, and Z directions are 7.322, 7.042, and 10.361 cm/s, respectively, occurring at 44 ms, 43 ms, and 41 ms. Overall, the pattern is $V_Z > V_X > V_Y$, with the Z direction exhibiting the most pronounced response. The vector-combined peak vibration velocity is 10.422 cm/s, also occurring at 41 ms, further indicating that the Z direction is the primary vibration direction under this blasting condition. The monitoring results also show that the maximum peak vibration velocity occurs in the first blasting section, which is related to the early initiation of the cutting holes and their poor free-face conditions.

To further evaluate the vibration response under different blasting conditions, 18 sets of field monitoring data from the K21 + 73–K21 + 98 section were analyzed statistically. As shown in Table 3, the monitored parameters included the distance from the blast center, the maximum charge per delay, and the peak vibration velocities in the axial, tangential, and vertical directions. The comprehensive monitoring results indicate that the three-dimensional vibration response of the diversion tunnel lining is dominated by vertical vibrations; therefore, subsequent safety assessments will focus on the peak vibration velocity in the Z-direction and its dominant frequency characteristics.

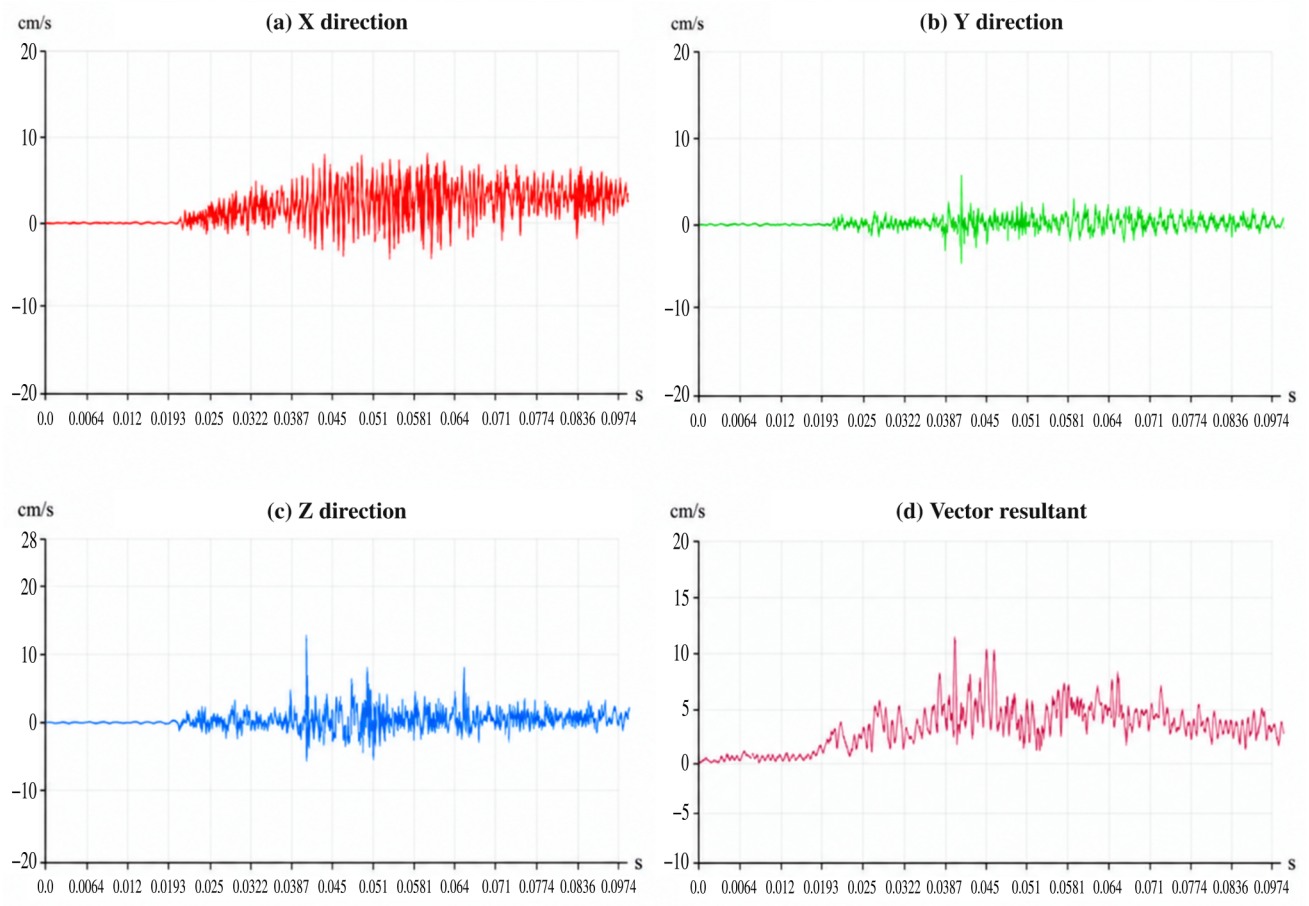


Figure 6. Typical vibration velocity waveforms measured during blasting.

Table 3. Summary of field monitoring vibration responses.

Monitoring Point	Chainage	Distance to Blast Source (m)	Maximum Charge per Delay (kg)	Axial Peak Particle Velocity (cm/s)	Tangential Peak Particle Velocity (cm/s)	Vertical Peak Particle Velocity (cm/s)
1	K21 + 73	53	11.3	4.112	5.531	7.208
2			11.2	5.052	4.757	8.247
3			11.4	7.322	7.042	10.361
4	K21 + 78	50	11.1	5.795	5.449	7.589
5			11.4	4.060	6.866	8.098
6			11.3	6.029	5.871	7.291
7	K21 + 83	47	11.2	6.438	8.920	9.714
8			11.3	5.634	7.299	9.101
9			11.4	7.898	6.510	8.576
10	K21 + 88	44	11.4	6.313	7.923	10.171
11			11.1	6.898	7.171	9.156
12			11.2	5.222	7.324	10.303
13	K21 + 93	41	11.3	9.407	10.263	11.181
14			11.4	9.179	8.010	9.642
15			11.2	8.959	9.051	10.877
16	K21 + 98	38	11.4	8.348	10.578	12.509
17			11.3	9.649	10.790	12.098
18			11.1	7.098	8.139	10.498

According to the Safety Regulations for Blasting (GB 6722-2014), when the dominant frequency of blasting vibration satisfies 10 Hz < f ≤ 50 Hz and the peak particle velocity (PPV) exceeds 10 cm/s, it is considered to exceed the specified limits. Among the 18 sets of monitoring results, 4 sets met the over-limit conditions, accounting for 22.22%; additionally, one set of monitoring data showed a PPV exceeding 9.5 cm/s within the same frequency range, accounting for 5.56%, indicating a state approaching the critical limit for safety control. At the same time, the dominant blasting frequency at the site differs significantly from the natural frequency range of 5–15 Hz for ordinary hydraulic tunnels mentioned in the original text, suggesting a low risk of direct resonance; however, the relatively high peak vibration velocity under certain operating conditions remains a major safety control issue.

As shown in Figure 7, these are the measured peak particle velocity and dominant frequency of vertical vibration.

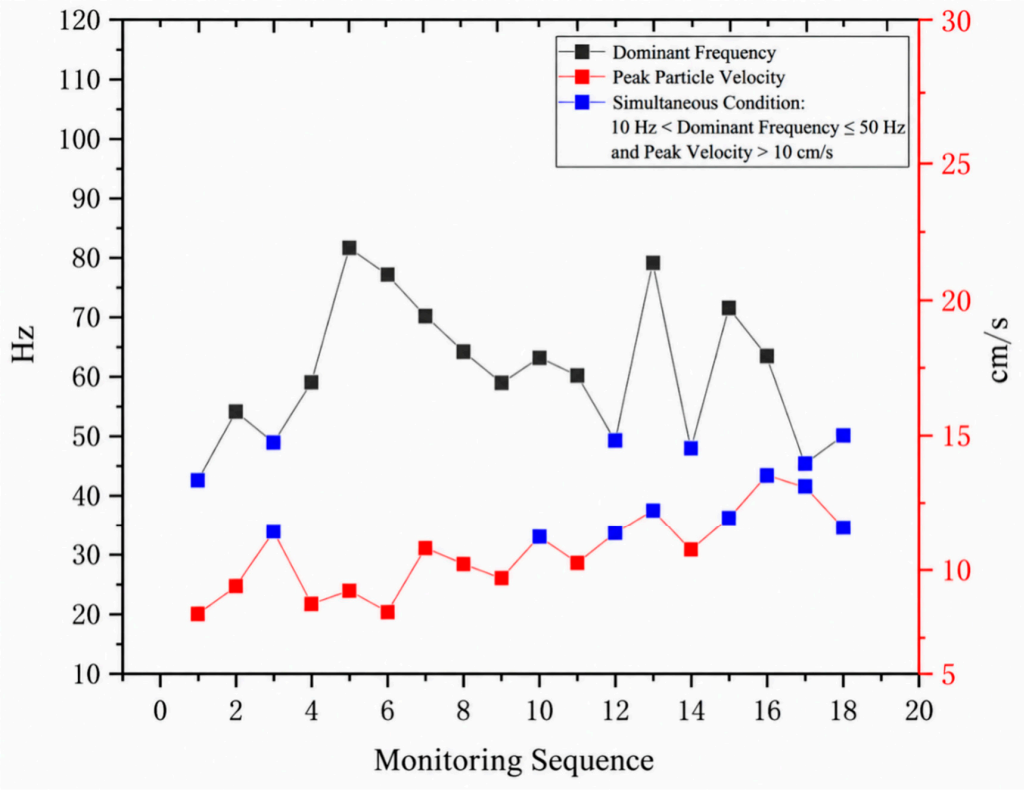


Figure 7. Measured peak particle velocity and dominant frequency of vertical vibration.

Previous studies have shown that blast-induced vibration is characterized by pronounced energy attenuation during propagation and that its dynamic effects are also closely related to vibration-frequency characteristics [20,21]. In summary, field monitoring indicates that blasting in the newly constructed tunnel had a significant transient vibration effect on the adjacent existing water diversion tunnel. The Z-direction was the primary vibration direction, and some blasting conditions exceeded or approached the regulatory control limits. Since field monitoring primarily reflects vibration velocity on the structure surface and cannot further reveal the dynamic response within the surrounding rock–lining system, the above monitoring results will serve as the experimental basis for subsequent numerical model validation and further dynamic response analysis.

3.2. Validation of Numerical Model

To verify the reliability of the numerical model's calculation results, the monitoring point on the right wall of the diversion tunnel at K21 + 73 was selected as the validation

location. The calculated results from the numerical model at the corresponding position were then compared with the field measurement data. The verification first focused on the time-history response of the vibration velocity in the Z-direction to compare the consistency between the numerical simulation and field monitoring results regarding the vibration response process and peak characteristics.

As shown in Figure 8, the numerical simulation and field measurements exhibit a good overall agreement in the time-history characteristics of the Z-direction vibration velocity. The peak Z-direction vibration velocity measured on-site was 10.361 cm/s, while the numerical simulation result was 10.815 cm/s, indicating that the numerical model can adequately reflect the main vibration response characteristics at this monitoring location.

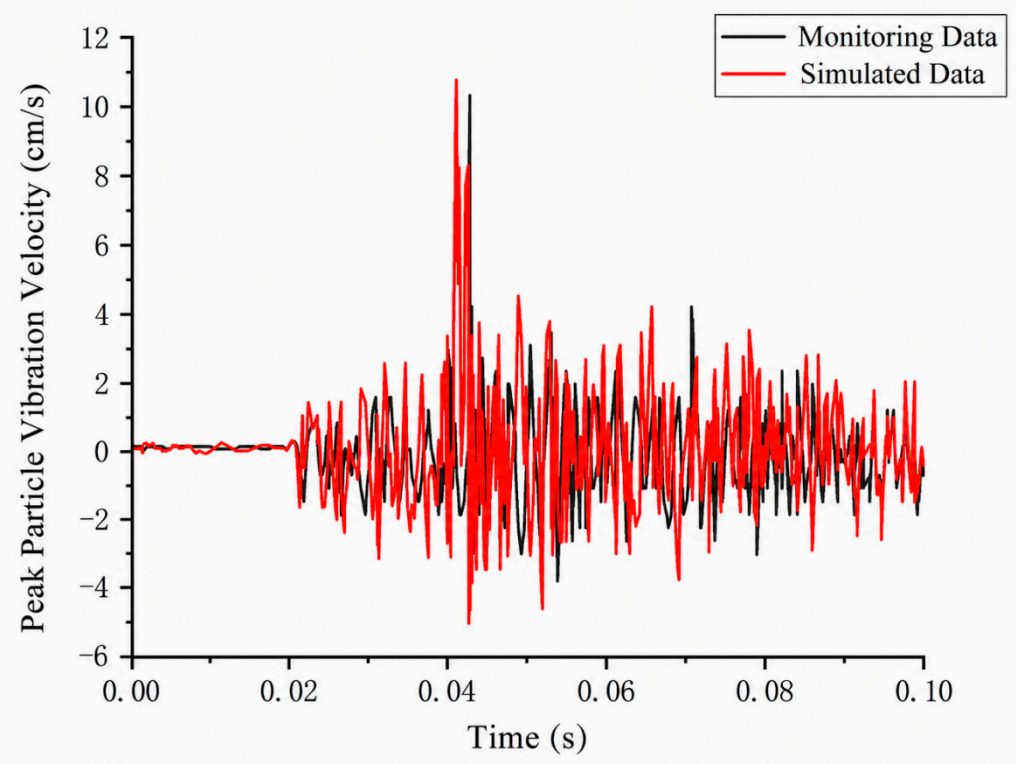


Figure 8. Comparison of measured and simulated Z-direction vibration velocities at K21 + 73.

To further quantitatively evaluate the calculation accuracy of the model, the peak vibration velocities in the X, Y, and Z directions were compared; the results are presented in Table 4.

Table 4. Comparison of measured and simulated peak particle velocities.

Direction	Measured PPV (cm/s)	Simulated PPV (cm/s)	Absolute Error (cm/s)	Relative Error (%)
X	7.322	7.753	0.431	5.89
Y	7.042	7.258	0.216	3.07
Z	10.361	10.815	0.454	4.38

Table 4 shows that the three-dimensional peak vibration velocities obtained from field measurements and numerical simulations exhibit the distribution characteristic of $V_Z > V_X > V_Y$, which is consistent with the main vibration direction identified through field monitoring. The relative errors in the X, Y, and Z directions are 5.89%, 3.07%, and 4.38%, respectively, with the relative error in the Z direction being 4.38%. Overall, the numerical simulation results agree well with the field monitoring data, indicating that the established

numerical model can reasonably reflect the vibration response of the adjacent existing water conveyance tunnel under blasting effects. This model can serve as a computational basis for subsequent dynamic response analysis.

3.3. Dynamic Response Characteristics of the Existing Diversion Tunnel

3.3.1. Spatial Distribution of Blast-Induced Vibration Along the Crossing Section

After completing the numerical model validation, the blasting dynamic response in the K21 + 104–K21 + 166 intersection section was calculated. Monitoring points were set at 10 m intervals along the arch waist of the existing diversion tunnel to extract the dominant vertical vibration frequency and peak vibration velocities in the X, Y, and Z directions at each location, thereby analyzing the spatial distribution characteristics of blasting vibrations within the intersection-affected zone.

As shown in Table 5, the simulation results indicate that blasting vibration responses at different locations vary significantly. As shown in Figure 9, the vertical dominant frequency in the intersection section generally ranges from approximately 40 to 80 Hz, and peak vibration velocities in all three directions exhibit certain fluctuations depending on location. Among these, the Z-direction vibration response is relatively prominent, with peak vibration velocities exceeding 10 cm/s at some locations. According to Table 5, higher vibration responses mainly occur in the middle and adjacent areas of the intersection section; specifically, the peak Z-direction vibration velocity at the monitoring point near K21 + 134 reaches 15.773 cm/s, the highest value among the simulated results. This indicates that the area adjacent to the intersection requires special attention regarding blasting vibrations.

Table 5. Summary of blasting simulation vibration monitoring data for the tunneling section of K21 + 104~K21 + 166.

Monitoring Point	Chainage	Vertical Dominant Frequency (Hz)	Vx (cm/s)	Vy (cm/s)	Vz (cm/s)
1	K21 + 104	48.38	5.648	7.433	10.411
2		51.23	6.275	6.975	13.594
3		49.31	5.834	6.721	10.217
4	K21 + 114	62.53	6.537	9.457	14.792
5		49.94	6.459	8.476	9.812
6		52.11	6.824	7.471	9.315
7	K21 + 124	73.61	8.432	8.317	13.216
8		55.29	7.479	10.122	12.338
9		62.41	7.821	7.651	9.251
10	K21 + 134	67.66	8.612	12.421	14.245
11		77.11	9.218	11.131	15.773
12		69.21	8.417	10.371	12.132
13	K21 + 144	63.24	8.375	11.278	14.886
14		78.44	8.681	8.934	13.296
15		71.33	7.172	9.421	12.152
16	K21 + 155	76.39	7.462	11.713	14.893
17		63.22	6.812	9.472	14.816
18		58.32	7.261	8.191	11.021
19	K21 + 166	51.36	8.163	8.437	12.977
20		47.51	6.921	7.199	9.851
21		46.33	6.276	6.702	10.663

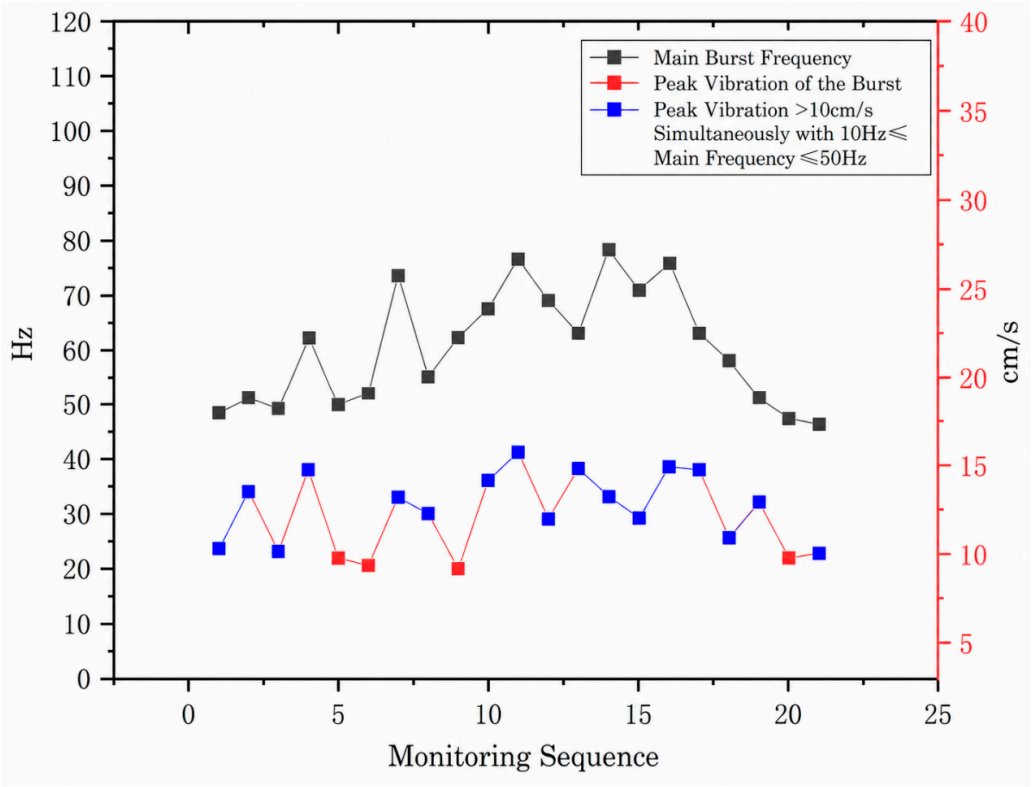


Figure 9. Distribution of vertical dominant frequency and peak particle velocity along the crossing section.

By combining the vertical dominant frequency and peak vibration velocity for safety evaluation, it can be observed that the vibration safety status varies at different locations within the crossing section. According to the relevant control requirements of the Blasting Safety Code (GB 6722-2014), the simulation results from the original paper indicate that approximately 9.52% of the working conditions are approaching the critical safety control state, while another 14.29% of the working conditions exceed the corresponding safety control limits when evaluated comprehensively based on the dominant frequency and peak vibration velocity. This suggests that under the current blasting parameters, there remains a risk of localized excessive vibration in the existing water diversion tunnel crossing area.

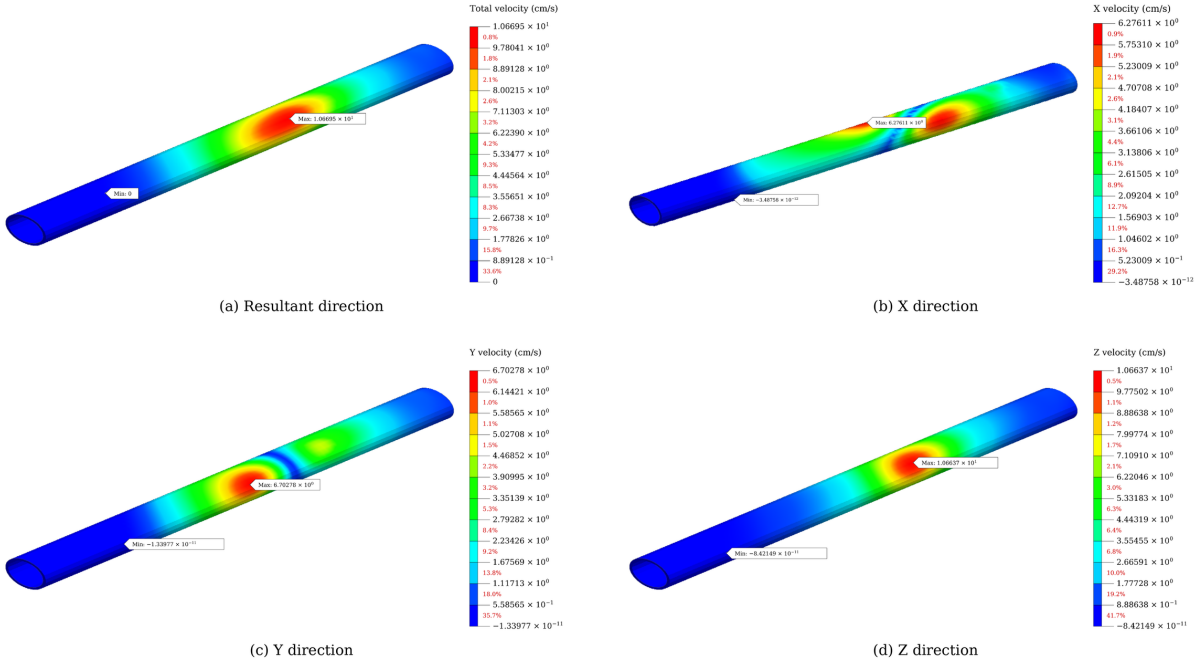
Overall, the spatial variation in PPV also reflects the attenuation characteristics of blast-induced vibration during propagation, which have been widely considered in tunnel blasting studies [22]; blasting vibration exhibits significant spatial non-uniformity along the K21 + 104–K21 + 166 intersection section; the dominant frequencies and peak vibration velocities vary across different monitoring locations, and the areas adjacent to the intersection show higher vibration responses. The above results reveal the spatial non-uniformity of vibration responses in the intersecting section. Considering that K21 + 166 is the location of spatial intersection and the minimum-clearance control point between two tunnels, this critical structural location was subsequently selected for further analysis of the time-history responses of lining vibration velocity, displacement, and stress.

Although a higher peak local vibration velocity was observed near K21 + 134, K21 + 166 is representative in terms of geometric spatial relationship and structural safety; therefore, it was selected as the location for subsequent structural dynamic response analysis.

3.3.2. Vibration Velocity Response and Temporal Evolution

Based on the analysis of the overall vibration response in the crossing section, the tunnel crossing node was further selected as the research object to analyze the vibration

velocity response of the existing lining of the diversion tunnel. As shown in Figure 10, numerical calculations yielded peak vibration velocities of 6.276, 6.702, and 10.663 cm/s in the X, Y, and Z directions, respectively, with a vector-combined peak value of 10.669 cm/s. Among the three directions, the Z-direction exhibited the most significant vibration response; moreover, the magnitude of the vector-combined peak and the location of maximum response were both close to those in the Z-direction, indicating that the Z-direction plays a dominant role in the overall vibration response at this location. This variation pattern is consistent with the field monitoring results.



(a) Resultant direction (b) X direction

(c) Y direction (d) Z direction

Figure 10. Distribution of peak particle velocity (PPV) in axial, tangential, and vertical directions.

Given that the vibration response in the Z-direction is the most pronounced, the evolution of the vibration velocity field in the lining along the Z-direction at different times was further analyzed. As shown in Figure 11, at t = 12 ms, higher vibration velocities first appeared in a localized area on the explosion-facing side near the blast source; the affected region was small, and the velocity gradient was significant. By t = 18 ms, the vibration response gradually spread along the axial and circumferential directions of the tunnel, leading to a noticeable velocity difference between the explosion-facing side and the opposite side. At t = 24 ms, local vibration responses intensified due to the propagation, superposition, and reflection of various blasting stress waves at the lining interface and tunnel boundaries. By t = 35 ms, the influence range of vibrations reached its maximum, with the most pronounced velocity gradient between the explosion-facing side and the opposite side; overall vibration intensity peaked during this process.

Subsequently, the vibration response gradually entered the decay phase. At t = 42 ms, the high-vibration velocity region significantly contracted, and the peak vibration velocity began to decrease; by t = 55 ms, the high-vibration velocity region had largely disappeared, and the velocity field became uniform and gentle. Overall, the vibration velocity of the lining in the existing diversion tunnel under blasting action exhibited a temporal evolution characterized by local excitation, propagation, reflection superposition, peak formation, and eventual gradual decay, with the Z-direction being the primary direction of vibration response.

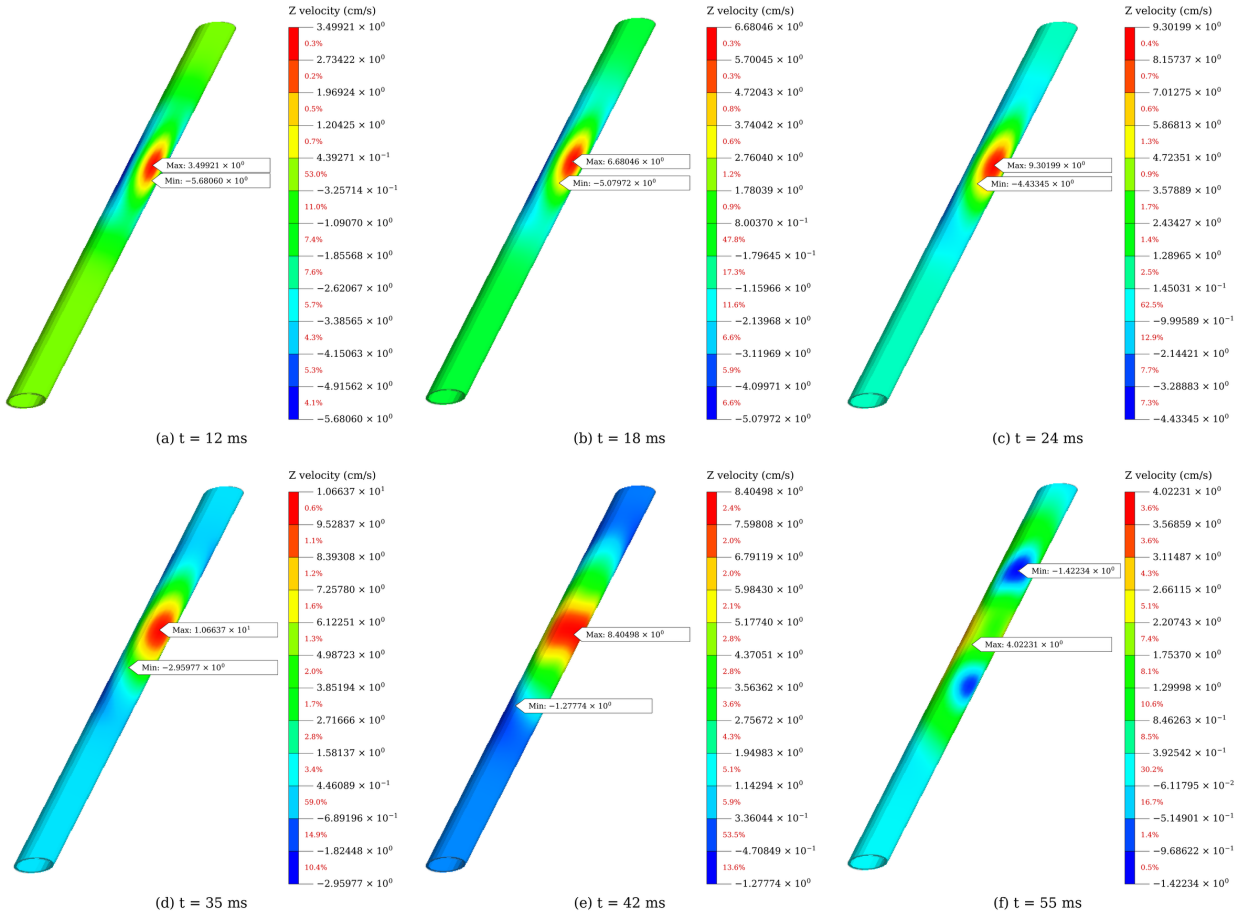


Figure 11. Contour plots of peak particle velocity (PPV) in the vertical (Z) direction at different time steps.

3.3.3. Displacement Response and Temporal Evolution

Based on the analysis of vibration velocity response, the displacement response of the lining in an existing water diversion tunnel under blasting action was further investigated. Numerical simulation results show that the lining displacement field exhibits distinct stage-wise evolutionary characteristics as the blasting vibration propagates.

As shown in Figure 12, in the initial stage of blasting (t = 10 ms), minor displacements appear first in local areas of the lining, indicating that the blasting stress wave causes local structural deformation upon reaching the lining. By t = 20 ms, as the stress wave continues to propagate and energy accumulates, the affected area of displacement gradually expands, and the peak displacement increases accordingly. When the time reaches 27 ms and 38 ms, the displacement field develops further due to the reflection and superposition of the stress wave at the lining interface and tunnel boundaries, leading to a continuous increase in local negative displacement. By t = 47 ms, the negative displacement response and its affected area become significantly stronger, marking a relatively pronounced stage of lining deformation.

From t = 56 ms onward, the displacement response evolves gradually from negative to positive displacement. Its spatial distribution differs significantly from that during the earlier negative-displacement phase, indicating a certain degree of positive-negative asymmetry in the lining displacement response under blasting dynamic effects. Numerical calculations show that the maximum lining displacement is 0.79 mm. According to the Technical Code for Safety Monitoring of Hydraulic Tunnel Structures (SL 764-2018) [23], this displacement remains within the allowable safety range. Overall, the lining displace-

ment under blasting undergoes a dynamic process involving local minor deformation, expansion of the affected area, increase in peak displacement, and subsequent transition between positive and negative displacements. This indicates that blasting vibrations have a notable transient deformation effect on existing water diversion tunnels; however, the calculated displacement does not exceed the corresponding safety control limits. As shown in Figure 13, the cloud chart of maximum positive displacement in the Z direction at a given moment is presented.

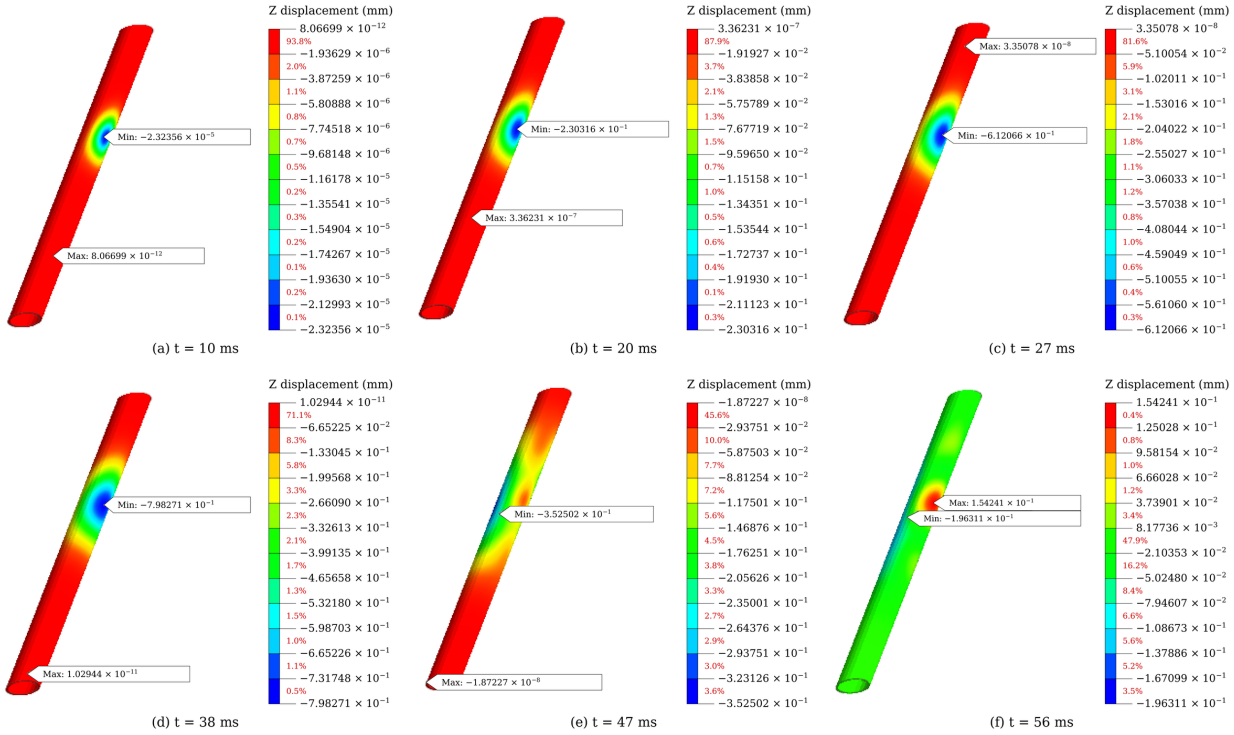


Figure 12. Contour plot of maximum negative displacement in the Z-direction at a given time step.

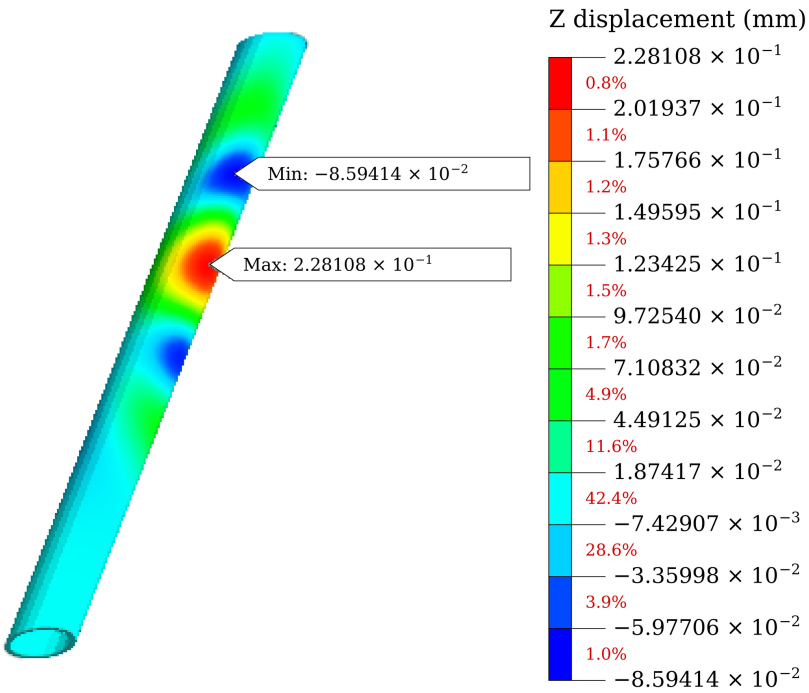


Figure 13. Contour plot of maximum positive displacement in the Z-direction at a given time step.

3.3.4. First Principal Stress Response and Temporal Evolution

Based on the analysis of vibration velocity and displacement responses, the dynamic response of the first principal stress in the lining of an existing water diversion tunnel under blasting is further investigated. After the blasting stress wave propagates to the lining, it causes the first principal stress field to change continuously over time, leading to stress concentration in certain regions. To reveal its evolutionary characteristics, the distribution of the first principal stress at different time nodes is extracted for analysis.

As shown in Figure 14, during the initial stage of blasting (t = 12 ms), a peak value of the first principal stress appears first in a local area of the lining, forming a transient stress concentration. By t = 18 ms, as the stress wave continues to propagate within the lining, the range of stress response gradually expands, and both the peak magnitude and spatial distribution change accordingly. In the period from t = 23 to 34 ms, the stress wave reflects at the lining interface and tunnel boundary and superimposes with stress waves traveling along different paths, further expanding the first principal stress field while causing noticeable fluctuations in local peak values. By t = 44 ms, the scope of stress influence continues to expand, and the local stress concentration effect intensifies further.

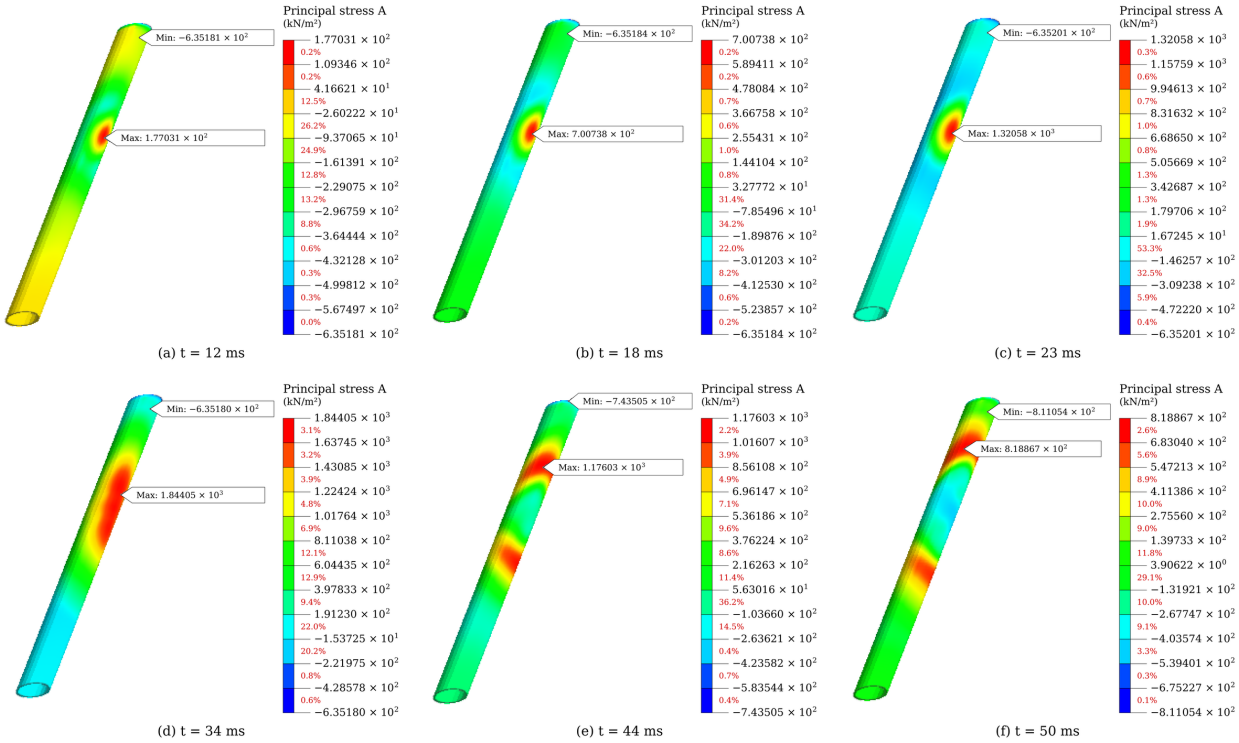


Figure 14. Contour plot of maximum principal stress in the Z-direction at a given time step.

Subsequently, as the blasting vibration energy gradually dissipates, the response of the first principal stress begins to decay. By t = 50 ms, the stress peak decreases, and the spatial distribution becomes progressively smoother, indicating that the lining's stress response enters a stage of decaying stabilization. Overall, the first principal stress undergoes a phased evolutionary process involving local stress concentration, expansion of the response range and peak fluctuations, followed by subsequent decay and stabilization.

Numerical calculations show that the maximum stress in the lining of this diversion tunnel is 1.84 MPa, which is lower than the cracking threshold of C30 concrete (2.01 MPa) and has not reached the critical cracking condition, though it is close to this limit. Therefore, under the current blasting conditions, the lining as a whole remains within the corresponding safety control range; however, local stress concentration and its dynamic evolution still require close attention.

3.4. Identification and Quantification of Influencing Factors

Based on the aforementioned field monitoring and numerical simulation results, the influencing factors of blasting vibration were screened according to the action process of blasting seismic waves: "generation—propagation—structural response". During the generation stage of blasting seismic waves, the total explosive charge, maximum single-blast charge, maximum charge in cut holes, number of delay times, and number of blast holes were considered. Among these, charging parameters directly affect the intensity of blasting energy release, while the number of delay times and blast holes influence the rhythm and spatial distribution of energy release. In the propagation stage, the distance from the explosion center was selected, as it directly affects the propagation and attenuation of blasting vibration waves in the surrounding rock medium. Ultimately, six parameters—total explosive charge, maximum single-blast charge, maximum charge in cut holes, distance from the explosion center, number of delay times, and number of blast holes—were identified as influencing factors, and blasting vibration responses were characterized by three indicators: dominant frequency, vibration velocity, and vibration duration. The original paper further explains that this study focuses on adjustable construction parameters, and geological conditions were not included as independent variables in the analysis.

The entropy-weight method was used to determine objective indicator weights based on data dispersion, whereas gray relational analysis was employed to quantify the relational degree between the blasting parameters and vibration responses [24,25]. The entropy weight-gray relational analysis method was employed to quantify the degree of correlation between various blasting parameters and vibration response indicators; the results are presented in Table 6.

Table 6. Entropy-weighted gray relational degrees between blasting parameters and vibration responses.

System Characteristic Variable	Gray Weighted Relational Degree of Relevant Factors					
	Total Charge	**Maximum Charge per Delay**	**Maximum Charge in Cut Holes**	**Distance to Blast Source**	**Number of Delay Intervals**	**Number of Blast Holes**
Dominant frequency	0.0744	0.0755	0.1017	0.1167	0.0540	0.1090
Peak particle velocity	0.1277	0.1298	0.1390	0.2005	0.0600	0.0797
Vibration duration	0.0692	0.0703	0.1135	0.1140	0.0578	0.1224
Total	0.2713	0.2756	0.3542	0.4312	0.1718	0.3111

For the dominant vibration frequency, the gray weighted correlation degrees of the blast center distance, number of blast holes, and maximum single-section charge of the cutting holes were 0.1167, 0.1090, and 0.1017, respectively, which were higher than those of other parameters. For vibration velocity, blast center distance had the highest correlation degree at 0.2005, followed by the maximum single-section charge of the cutting holes at 0.1390; the correlation degrees for maximum single-section charge and total charge were 0.1298 and 0.1277, respectively. For vibration duration, the correlation degrees of the number of blast holes, blast center distance, and maximum single-section charge of the cutting holes were 0.1224, 0.1140, and 0.1135, respectively, indicating relatively high degrees of correlation.

Based on the three vibration response indicators, the cumulative gray weighted correlation degrees of various factors are as follows: distance from the explosion center

(0.4312) > maximum charge per delay in the cutting holes (0.3542) > number of blast holes (0.3111) > maximum charge per delay (0.2756) > total charge amount (0.2713) > number of delay times (0.1718). The results show that the distance from the explosion center has the highest correlation with overall blasting vibration response; however, it is mainly constrained by the spatial relationship between the two tunnels, leaving limited room for adjustment in engineering applications. In contrast, maximum charge per delay in the cutting holes exhibits a high correlation with the dominant vibration frequency, vibration velocity, and vibration duration, making it an important parameter that can be controlled at the source of blasting. The number of blast holes, maximum charge per delay, and total charge amount also have significant effects and can serve as the main control variables for optimizing subsequent blasting parameters. The number of delay times shows a relatively low comprehensive correlation under the conditions of this study.

The above analysis indicates that blasting vibrations in existing water diversion tunnels are jointly influenced by multiple factors such as blasting energy release, propagation distance, and blast hole arrangement. When spatial conditions cannot be altered, subsequent optimization should focus on adjustable parameters such as maximum charge per delay in the cutting holes, number of blast holes, maximum charge per delay, and total charge amount, while implementing coordinated control based on the delay sequence. This provides a basis for the targeted optimization of blasting schemes.

3.5. Optimization of Blasting Parameters and Vibration Control

3.5.1. Optimization Strategy and Parameter Adjustment

According to the entropy weight–gray relational analysis results in Section 3.4, the explosion center distance has the highest comprehensive correlation degree (0.4312), indicating that propagation distance significantly affects blasting vibration response. However, the spatial relationship between the two tunnels is largely determined during construction, limiting the engineering adjustability of the explosion center distance. Therefore, under given spatial conditions, blasting scheme optimization focuses on controllable parameters such as the maximum charge per delay for cutting holes, the maximum charge per delay, the number of blast holes, and the total charge amount, while using the delayed detonation sequence as an auxiliary control measure.

Jia et al. [26] investigated the influence of free-surface conditions on tunnel blasting vibration attenuation, while Yan et al. [27] examined prediction methods for blast-induced peak particle velocity. To determine the maximum allowable charge per delay under the present crossing conditions, Sadovsky's empirical formula is used to relate peak particle velocity to the maximum charge per delay and the blast-source distance:

$$V = K\left(\frac{\sqrt[3]{Q}}{R}\right)^{\alpha}$$

In the formula, (V) is the peak particle vibration velocity (cm/s), (Q) is the maximum charge per delay (kg), (R) is the distance from the explosion center (m), and (K) and (α) are the site coefficient and attenuation index related to site conditions and blasting methods, respectively.

To determine the site coefficient K and attenuation index α applicable to the engineering conditions of this project, regression analysis was performed using 18 sets of field blasting vibration monitoring data obtained from the left tunnel's near-intersection section during the preliminary stage of the same project. These data correspond to blast center distances ranging from 12.8 to 21.1 m and can reflect the variation characteristics of blasting vibrations with respect to blast center distance and maximum single-blast charge amount as the new tunnel gradually approaches the existing water diversion tunnel. The monitored

parameters include blast center distance, maximum single-blast charge amount, and peak particle vibration velocities in the axial, tangential, and vertical directions; the specific data are presented in Table 7.

Table 7. Field monitoring data used for calibration of the Sadowski attenuation relationship.

Monitoring Point	Blast Center Distance (m)	Maximum Single-Segment Charge (kg)	Axial Vibration Velocity Vx (cm/s)	Tangential Vibration Velocity Vy (cm/s)	Vertical Vibration Velocity Vz (cm/s)
1	21.1	11.9	3.112	4.531	4.999
2	20.6	11.5	3.052	4.757	5.611
3	20.1	11.4	4.322	5.042	5.648
4	19.6	11.9	3.795	3.449	4.826
5	19.0	11.1	4.060	5.866	6.044
6	18.6	11.6	3.029	5.871	6.103
7	18.3	11.8	3.438	5.920	6.978
8	17.5	11.3	5.634	5.299	6.297
9	17.4	11.7	5.898	6.510	7.032
10	16.4	11.6	6.313	6.923	7.578
11	16.2	11.8	6.898	6.171	7.552
12	15.6	11.5	5.222	7.324	8.102
13	15.3	11.2	6.407	7.263	8.236
14	14.5	11.9	6.179	8.010	8.583
15	14.2	11.5	6.959	9.051	9.574
16	13.9	11.5	6.348	7.578	8.301
17	13.3	11.5	8.649	8.790	9.072
18	12.8	11.4	7.098	9.139	10.642

Taking the logarithm of both sides of the formula yields the function:

$$\ln V = \ln K + \alpha\left(\frac{1}{3}\ln Q - \ln R\right)$$

Let InV = Y, InK = A, = B, and 1/3ln$Q$ − ln$R$ = X; the resulting simple linear regression equation is:

$$y = A + Bx$$

A regression analysis using the least squares method was performed on 18 sets of field monitoring data, yielding:

$$Y = 1.38X + 4.73$$

Thus, it is determined that: α = 1.38, K = 113.5.

The fitted correlation coefficient R2 is 0.908, indicating that this empirical relationship can adequately describe the propagation and attenuation characteristics of blasting vibration under near-crossing conditions in this project. Therefore, the blasting vibration attenuation relationship for this project can be expressed as

$$V = 113.5\left(\frac{\sqrt[3]{Q}}{R}\right)^{1.38}$$

Previous research on buried pipelines has established blast-vibration control criteria by relating vibration velocity to structural response and material strength [28].

Field blasting and simulation results show that the main blasting frequency fluctuates within the range of 40–90 Hz. To ensure the safety of the adjacent diversion tunnel, the maximum allowable peak blasting vibration velocity is set at 10 cm/s. The minimum

distance between the two tunnels is 12.8 m, and the calculated maximum permissible charge per blast segment is Q = 10.67 kg. Therefore, under conditions of close-proximity construction, the maximum charge per blast segment should be controlled within 10.67 kg. This result further provides a quantitative control basis for optimizing the charge-related parameters identified in the aforementioned analysis of influencing factors.

Accordingly, the original three-step blasting plan was adjusted. For the upper bench, the energy concentration in the cutting zone was reduced by decreasing the number of cutting holes from 8 to 6; the maximum charge in cut holes was reduced from 3.6 kg to 2.7 kg, and the total charge for the upper bench was lowered from 28.2 kg to 24.0 kg by reducing the amount of explosives per hole. For the middle and lower benches, the charge per mucking hole was reduced from 0.60 kg to 0.45 kg, and the number of perimeter holes was appropriately increased to disperse the blasting energy and improve contour formation; the original burden distance of 700 mm and hole spacing of 1000 mm were maintained. Meanwhile, the number of delay initiation times for the upper bench was increased from 6 to 7 to weaken the superposition effect of vibration waves from different blast holes, while the cyclic advance length remained at 1.2 m.

After optimization, the maximum charge per segment is controlled at 7.656 kg, satisfying the condition: 7.656 kg < 10.67 kg.

This indicates that the optimized scheme meets the control requirements for the maximum charge per segment under near-crossover conditions. The specific optimized blasting parameters are listed in Table 8, and the optimization effects will be further verified through numerical simulation and field monitoring in Section 3.5.2.

Table 8. Optimized blasting parameters.

Section	Delay Time (ms)	Number of Blast Holes	Explosive Quantity (kg)
Upper Bench	0	6	2.7
	50	6	2.25
	100	6	1.8
	150	4	1.2
	200	20	5.25
	250	12	3.6
	300	32	7.2
Middle Bench	0	10	3
	50	12	3.6
	100	8	0.9
Lower Bench	0	9	2.7
	50	4	1.2
	100	34	7.656
	Grand Total	163	43.056
Grand Total	Single blast: 163 holes, total charge 43.056 kg.		

3.5.2. Verification of the Optimized Blasting Scheme

As shown in Figure 15, the optimized scheme for the K21 + 104–K21 + 166 intersection section was calculated using a validated numerical model. The peak vibration velocities in the X, Y, and Z directions at the intersection decreased from 6.276, 6.702, and 10.663 cm/s to 5.271, 5.557, and 8.696 cm/s, respectively, representing reductions of 16.01%, 17.08%, and 18.45%. This indicates that the optimized scheme can significantly reduce blasting vibration responses.

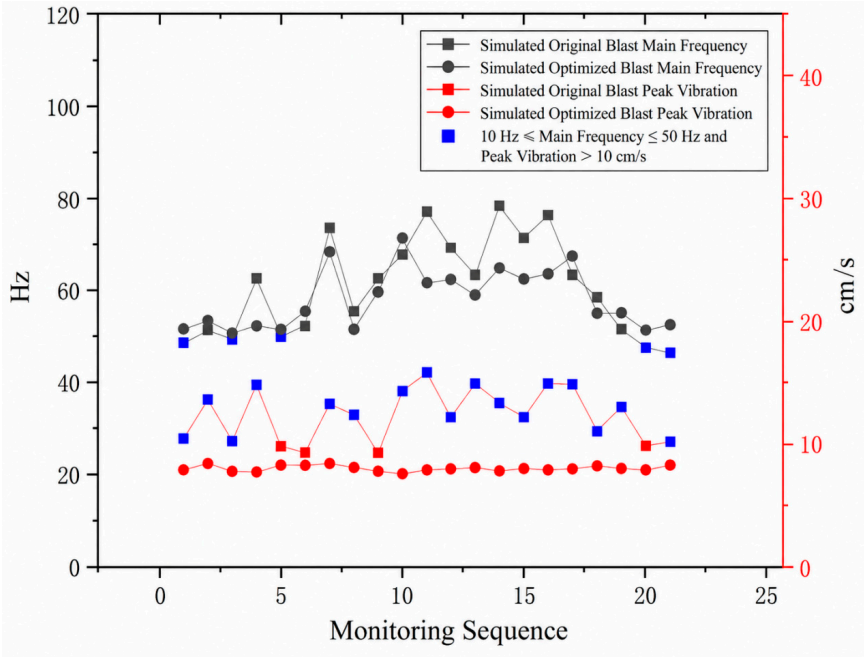


Figure 15. Comparison of simulated vertical dominant frequency and peak particle velocity before and after optimization.

Subsequently, a field trial explosion of the optimized scheme was conducted at K21 + 73. The measured peak vibration velocities in the X, Y, and Z directions were 6.513, 6.289, and 8.129 cm/s, respectively—representing decreases of 11.05%, 10.69%, and 21.54% compared to the pre-optimization monitoring results. The vibration reduction effect was most significant in the Z direction.

Based on this, the optimized blasting scheme was further applied to the K21 + 104–K21 + 166 intersection section, with on-site vibration monitoring carried out at 10 m intervals along the construction section. As shown in Figure 16, the monitoring results showed that blasting vibrations at all measurement points were effectively controlled after optimization. At K21 + 166, where the distance between the two tunnels is the smallest, the peak vibration velocities in the X, Y, and Z directions were 5.532, 5.901, and 8.352 cm/s, respectively.

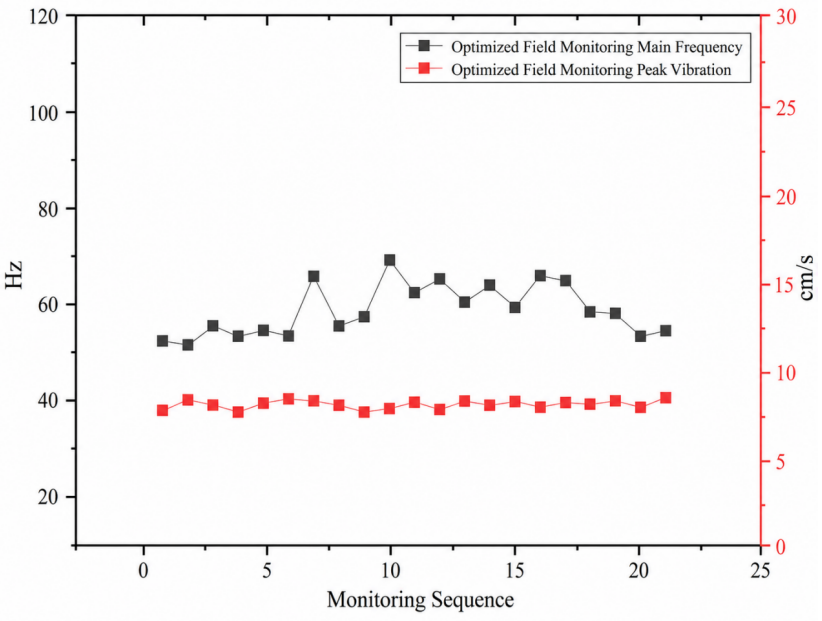


Figure 16. Field-monitored vertical dominant frequency and peak particle velocity after optimization.

On-site inspection revealed no structural damage to the adjacent diversion tunnel; the lining stress was 0.87 MPa, lower than the cracking threshold of C30 concrete at 2.01 MPa. Based on numerical simulations, on-site blasting tests, and actual construction monitoring data from the crossover section, the optimized scheme effectively reduced the blasting vibration response in the adjacent diversion tunnel while maintaining a 1.2 m cyclic advance rate and existing construction techniques. This confirms the vibration reduction effectiveness and engineering applicability of the scheme.

4. Conclusions

4.1. Limitations and Future Work

This study is based on the existing water diversion tunnel project adjacent to Miaolin Tunnel, and the applicability of the research conclusions under other geological conditions and cross-relationships still needs to be verified. The numerical model uses an equivalent triangular pressure load, which simplifies the actual hole geometry and blasting process. Model verification is mainly based on the vibration velocity comparison of representative measuring points, while the verification of other section positions and stress and displacement responses is still limited. In addition, the range of dose changes in attenuation regression samples is narrow, and gray correlation analysis and multi-parameter synchronous adjustment also make it difficult to fully distinguish the independent effects of various factors and optimization measures.Previous research has identified limitations in using entropy-derived weights for multicriteria decision-making [29]. Further sensitivity analysis is therefore needed to assess the robustness of the factor rankings obtained in this study.

In the future, monitoring data for different surrounding rock conditions, intersection spacing, and section locations can be expanded to strengthen the joint verification of vibration velocity time history and frequency characteristics; Conduct load, grid, and time step sensitivity analysis to gradually refine the numerical simulation of the blasting process; Combined with a wider range of monitoring samples and parameter control tests, the application scope of the attenuation relationship was examined, the vibration reduction contribution of various measures was evaluated, and the reliability and engineering applicability of the control method were improved.

4.2. Conclusions

Regarding the impact of blasting construction for a newly built tunnel on an adjacent existing water diversion tunnel, this paper conducts research by integrating field monitoring, numerical simulation, entropy weight-gray relational analysis, and blasting parameter optimization. The main conclusions are as follows:

(1) Field monitoring indicates that the peak three-dimensional vibration values near the water diversion tunnel generally follow the order $V_Z > V_X > V_Y$, with the maximum peak value in the Z direction reaching 10.361 cm/s. Among 18 sets of monitoring data, 22.22% of the working conditions exhibited excessive vibration velocity, and 5.56% were at a critical safety state, indicating a clear need for vibration control under the original blasting conditions.

(2) The established three-dimensional numerical model agrees well with the measured results, with the relative error in peak three-dimensional vibration velocity being less than 6%; the error in the Z direction was 4.38%. The vibration response in the intersection section shows significant spatial non-uniformity, with the Z direction dominating; the maximum displacement of the lining is 0.79 mm, and the maximum first principal stress is 1.84 MPa, both below the cracking threshold of 2.01 MPa for C30 concrete.

(3) Entropy weight-gray correlation analysis shows that the comprehensive correlation degree of all influencing factors is in the order of burst center distance (0.4312), maximum single-stage charge amount of grooved hole (0.3542), number of blasting holes (0.3111), maximum single-stage charge amount (0.2756), total charge amount (0.2713), and number of delayed explosion time (0.1718). Because of the limited adjustability of the explosion center distance, the maximum single-stage charge quantity of notched holes, the number of blasting holes, the maximum single-stage charge quantity, and the total charge quantity become the main optimization parameters.

(4) According to the blasting vibration attenuation relationship, the safety allowable maximum single-stage charge is 10.67 kg, which is controlled to 7.656 kg after optimization, and the total charge is 43.056 kg. Numerical simulation shows that the peak vibration velocity in the X, Y, and Z directions decreases by 16.01%, 17.08%, and 18.45%, respectively. In the field monitoring, the three-way peaks at K21 + 166 were 5.532, 5.901, and 8.352 cm/s; the lining stress was 0.87 MPa, and no structural damage was found, which verified the vibration reduction effect and engineering applicability of the optimized scheme.

Author Contributions: Conceptualization, S.W. and Q.F.; investigation, Q.F. and J.T.; writing—original draft preparation, J.T. and Q.F.; data curation, B.Y. All authors have read and agreed to the published version of the manuscript.

Funding: This research was funded by the Graduate Student Innovation Program of Chongqing University of Science and Technology, grant number YKJCX2520722.

Data Availability Statement: The original contributions presented in this study are included in the article. Further inquiries can be directed to the corresponding author.

Conflicts of Interest: The authors declare no conflicts of interest.

References

1. Liu, T.; Wang, L.W. Analysis and field measurement of vibration response induced by highway tunnel blasting on adjacent water diversion tunnels. *Tunn. Constr.* **2014**, *34*, 1113–1120.
2. Yang, Z.; Hu, Y.; Liu, M.; Li, P.; Yao, E.; Ma, C. Discussion on the discreteness of the attenuation parameters of the peak particle velocity induced by blasting. *Sensors* **2024**, *24*, 1355. [CrossRef] [PubMed]
3. Gao, Y.; Fu, H.; Rong, X.; Paneiro, G. Ground-borne vibration model in the near field of tunnel blasting. *Appl. Sci.* **2023**, *13*, 87. [CrossRef]
4. Zeng, X.; Zhang, X.; Zhou, X.; Duan, Y.; Chen, J. Prediction of tunnel blasting vibration velocity considering the influence of free surface. *Appl. Sci.* **2023**, *13*, 1373. [CrossRef]
5. Yang, J.H.; Lu, W.B.; Jiang, Q.H.; Yao, C.; Zhou, C.B. Frequency comparison of blast-induced vibration per delay for the full-face millisecond delay blasting in underground opening excavation. *Tunn. Undergr. Space Technol.* **2016**, *51*, 189–201. [CrossRef]
6. Ma, C.-Y.; Wu, L.; Sun, M.; Yuan, Q. Time-frequency analysis and application of a vibration signal of tunnel excavation blasting based on CEEMD-MPE-HT. *Shock Vib.* **2021**, *2021*, 6672942. [CrossRef]
7. Zhao, H.-B.; Long, Y.; Li, X.-H.; Lu, L. Experimental and numerical investigation of the effect of blast-induced vibration from adjacent tunnel on existing tunnel. *KSCE J. Civ. Eng.* **2016**, *20*, 431–439. [CrossRef]
8. Luo, Y.; Gong, H.; Qu, D.; Zhang, X.; Tao, Y.; Li, X. Vibration velocity and frequency characteristics of surrounding rock of adjacent tunnel under blasting excavation. *Sci. Rep.* **2022**, *12*, 8453. [CrossRef] [PubMed]
9. Han, G.; Li, M.; Mei, W. The stability analysis of blasting excavation in short distance on water diversion tunnel underpassing Jinduicheng Molybdenum Mine. *J. Vibroeng.* **2019**, *21*, 1139–1146. [CrossRef]
10. Du, X.; Xiao, Q.; Li, C.; Xiong, Q.; Yu, J. Researches on the influence of blasting of newly built tunnel on the existing tunnel structure with small cross angle. *Adv. Civ. Eng.* **2021**, *2021*, 1865694. [CrossRef]
11. Zhang, Y.; Zhang, J.; Wang, S.; Chen, Y. Controlling vibration speed in tunnel excavation using fine blasting method under complex environmental conditions. *Shock Vib.* **2021**, *2021*, 6060485. [CrossRef]
12. Guan, X.; Yao, Y.; Yang, N.; Xu, H.; Xin, B.; Li, B. Analysis of factors influencing vibration reduction and design optimization of damping holes in adjacent tunnel blasting. *Case Stud. Constr. Mater.* **2023**, *19*, e02448. [CrossRef]

13. Tao, T.; Wan, S.; Liu, L.; Pan, T. A method based on spectrum superposition for minimizing the hazards of blasting vibration. *KSCE J. Civ. Eng.* **2021**, *25*, 1670–1686. [CrossRef]
14. Zhou, J.; Gao, S.; Luo, P.; Fan, J.; Zhao, C. Optimization of blasting parameters considering both vibration reduction and profile control: A case study in a mountain hard rock tunnel. *Buildings* **2024**, *14*, 1421. [CrossRef]
15. *GB 6722-2014*; Safety Regulations for Blasting. Standards Press of China: Beijing, China, 2014.
16. Hu, Q.G.; Cui, W.F.; Gao, J.W.; Zhao, F.W.; Liang, Q.F. Blasting excavation and vibration monitoring design for diversion tunnel. *Adv. Mater. Res.* **2013**, *639*, 969–973. [CrossRef]
17. Zhang, X.B.; Liu, Q.S.; Tian, Y.C.; Su, X.J.; Zhong, Y.Q. Monitoring and controlling technology for blasting vibration of Houci Tunnel. *Sci. Technol. Eng.* **2016**, *16*, 113–120.
18. Jimeno, C.L.; Jimeno, E.L.; Carcedo, F.J.A. *Drilling and Blasting of Rocks*; CRC Press: Boca Raton, FL, USA, 1995.
19. Zhang, Y.C. An Equivalent Approach for Acting Blasting Load in Dynamic Numerical Simulation of Blasting Vibration. *Chin. J. Undergr. Space Eng.* **2012**, *8*, 56–64.
20. Li, H.T.; Lu, W.B.; Shu, D.Q.; Yang, X.G.; Yi, C.P. Study on Energy Attenuation Law of Blast-Induced Seismic Waves. *Chin. J. Rock Mech. Eng.* **2010**, *29*, 3364–3369.
21. Liu, D.; Zhao, X.; Gao, J.; Xue, B.; Wu, X.; Hu, S.; Chen, F. Numerical study on the relationship between the dominant frequency of blasting vibration and the development of plastic zone in cylindrical charge. *Geofluids* **2022**, *2022*, 9017792. [CrossRef]
22. Fei, H.L.; Zhang, X.Z.; Yang, Z.G. The prediction and control research on the attenuation law of blasting vibration peak velocity in Daiyuling Tunnel. *Adv. Mater. Res.* **2013**, *838–841*, 1429–1434. [CrossRef]
23. *SL 764-2018*; Technical Specification for Safety Monitoring of Hydraulic Tunnels. China Water & Power Press: Beijing, China, 2018.
24. Zhu, X.Y.; Xiao, N.; Jiang, Q.Q. Evaluation and Simulation Analysis of Influencing Factors of Stray Current in Urban Rail Transit Based on the Entropy Weight Method. *Auto Wkly.* **2026**, *1*, 38–40.
25. Dong, P.F.; Tang, K. Stability Analysis of Highway Soft Soil Subgrade Slopes Based on the Grey Relational Method. *Transp. Sci. Technol. Manag.* **2025**, *6*, 92–94.
26. Jia, B.; Zhou, L.; Cui, J.; Chen, H. Attenuation model of tunnel blast vibration velocity based on the influence of free surface. *Sci. Rep.* **2021**, *11*, 21077. [CrossRef] [PubMed]
27. Yan, Z.X.; Yan, L.; Jiang, P.; Wang, H.Y. Prediction methods for blasting-induced ground vibration velocity. *J. Vib. Shock* **2010**, *29*, 179–182. [CrossRef]
28. Shi, C.; Zhao, Q.; Lei, M.; Peng, M. Vibration velocity control standard of buried pipeline under blast loading of adjacent tunnel. *Soils Found.* **2019**, *59*, 2195–2205. [CrossRef]
29. Žižović, M.; Albijanić, M. An implementation of the entropy method for determining weighing coefficients in a multicriteria optimization of public procurements. *Spectr. Eng. Manag. Sci.* **2025**, *3*, 28. [CrossRef]

Disclaimer/Publisher's Note: The statements, opinions and data contained in all publications are solely those of the individual author(s) and contributor(s) and not of MDPI and/or the editor(s). MDPI and/or the editor(s) disclaim responsibility for any injury to people or property resulting from any ideas, methods, instructions or products referred to in the content.